

Tyrosine kinase receptors as molecular targets in pheochromocytomas and paragangliomas

Clarissa A. Cassol¹, Daniel Winer¹, Wei Liu², Miao Guo², Shereen Ezzat^{2,3}, and Sylvia L. Asa^{1,2}

¹Department of Pathology, University Health Network, Toronto, Ontario, Canada

³Department of Internal Medicine, University Health Network, Toronto, Ontario, Canada

²Ontario Cancer Institute, University Health Network, Toronto, Ontario, Canada

Abstract

Pheochromocytomas and paragangliomas are neuroendocrine tumors shown to be responsive to multi-targeted tyrosine kinase inhibitor treatment. Despite growing knowledge regarding their genetic basis, the ability to predict behavior in these tumors remains challenging. There is also limited knowledge of their tyrosine kinase receptor expression and whether the clinical response observed to the tyrosine kinase inhibitor Sunitinib relates only to its anti-angiogenic properties or also due to a direct effect on tumor cells.

To answer these questions, an *in vitro* model of sunitinib treatment of a pheochromocytoma cell line was created. Sunitinib targets (VEGFRs, PDGFRs, C-KIT), FGFRs and cell cycle regulatory proteins were investigated in human tissue microarrays. SDHB immunohistochemistry was used as a surrogate marker for the presence of succinate dehydrogenase mutations. The *FGFR4*G388R SNP was also investigated.

Sunitinib treatment *in vitro* decreases cell proliferation mainly by targeting cell cycle, DNA metabolism, and cell organization genes. FGFR1, -2 and -4, VEGFR2, PDGFR α and p16 were overexpressed in primary human pheochromocytomas and paragangliomas. Discordant results were observed for VEGFR1, p27 and p21 (overexpressed in paragangliomas but underexpressed in pheochromocytomas); PDGFR β , Rb and Cyclin D1 (overexpressed in paragangliomas only) and FGFR3 (overexpressed in pheochromocytomas and underexpressed in paragangliomas). Low expression of C-KIT, p53, Aurora Kinase A and B was observed. Nuclear FGFR2 expression was associated with increased risk of metastasis (odds ratio [OR]=7.61; p=0.008), as was membranous PDGFR α (OR= 13.71, p=0.015), membranous VEGFR1 (OR=8.01; p=0.037), nuclear MIB1 (OR=1.26, p=0.008) and cytoplasmic p27 (OR=1.037, p=0.030). FGFR3, VEGFR2 and C-KIT levels were associated with decreased risk of metastasis.

Users may view, print, copy, and download text and data-mine the content in such documents, for the purposes of academic research, subject always to the full Conditions of use:http://www.nature.com/authors/editorial_policies/license.html#terms

Address correspondence to: Dr. Sylvia L. Asa, Department of Pathology, University Health Network, 200 Elizabeth Street, 11th Floor, Toronto, Ontario M5G 2C4, Telephone: 416-340-4802, Facsimile: 416-340-5517, sylvia.asa@uhn.ca.

Disclosure/Conflict of interest:

The authors declare no conflict of interest.

Supplementary Information accompanies the paper on the Modern Pathology website (<http://www.nature.com/modpathol>).

We provide new insights into the mechanistic actions of sunitinib in pheochromocytomas and paragangliomas and support current evidence that multitargeted tyrosine kinase inhibitors might be a suitable treatment alternative for these tumors.

Keywords

pheochromocytomas; paragangliomas; tyrosine kinase receptors; sunitinib

INTRODUCTION

Pheochromocytomas and paragangliomas are tumors of neural crest-derived endocrine cells throughout the distribution of the sympathetic and parasympathetic nervous system (1). The discovery of succinate dehydrogenase (*SDH*) mutations as a frequent underlying cause of paragangliomas in the year 2000 has launched a phase of accelerated gene discovery in these tumors; it is now known that a genetic predisposition is present in almost 30% of cases (2). However, despite growing knowledge of their genetics, the ability to predict behavior in these tumors remains challenging. Numerous factors have been associated with malignancy, including the presence of *SDHB* mutations (2), high proliferative index (3–4) and tumor size and location (5); however the only accepted criterion of malignancy is the presence of distant metastasis (1).

When malignant, pheochromocytomas and paragangliomas do not usually respond to traditional therapies. Recent reports of successful treatment of malignant pheochromocytoma/paraganglioma with the multi-targeted tyrosine kinase inhibitor (TKI) sunitinib provided clinical evidence that receptor tyrosine kinases (RTKs) might be involved in the development or progression of these tumors (6–7). RTKs and their ligands are known to be mutated or overexpressed in a variety of endocrine malignancies, including thyroid (8, 9), pituitary (10), pancreas (11), pheochromocytomas (3, 12–15) and paragangliomas (16). Single nucleotide polymorphisms (SNPs) in RTK genes may also play a role in development or progression of tumors, as is the case with the common *FGFR4* G388R SNP (17).

Since therapeutic response to TKIs in tumor models has been shown to be due not only to an anti-angiogenic effect but also to a direct effect on tumor cells (18, 19), we decided to investigate this possibility by creating an *in vitro* model of Sunitinib treatment using a mouse pheochromocytoma cell line (MPC 4/30), (20). In addition, tissue microarrays from human tumors were constructed and stained with antibodies against the main Sunitinib potential targets (VEGFRs, PDGFRs, C-KIT), as well as other RTKs (FGFRs) that might be related to the development of therapeutic resistance (11, 21). Following our initial observations that *in vitro* treatment of pheochromocytoma cells results in significantly altered expression of cell-cycle regulatory proteins, we further expanded the tissue microarray immunohistochemistry panel to include cell cycle regulatory proteins (Cyclin D1, Rb, p16, p21, p27, p53, MIB1, Aurora A and B). *SDHB* immunohistochemistry was used as a surrogate maker for *SDH* mutations (22) and genotyping for the common *FGFR4* G388R polymorphism was performed in order to assess a possible influence of this SNP on the development and progression of these tumors (17, 23).

MATERIALS AND METHODS

In vitro studies - Sunitinib treatment of a mouse pheochromocytoma cell line

The MPC 4/30 mouse pheochromocytoma cell line was kindly provided by Dr A. Tischler (Tufts Medical Center, Boston, MA, USA) and maintained as previously described (20). Sunitinib malate 100mg was purchased from Sequoia Research Products Ltd (Pangbourne, UK, SRP01785s,) and dissolved in dimethyl sulfoxide to obtain a 25 mM solution. Cells were cultured on 10 cm plates. After trypsinization, 2 million cells were plated, grown in supplemented medium for 24 h, starved in serum-free medium for 24 h, then treated with sunitinib malate in different concentrations (0 uM, 2.5 uM and 5.0 uM) for 72 hours. Cells were then trypsinized and divided for flow cytometry and RNA expression analysis. For flow cytometry, 1 to 3×10^6 cells were washed with PBS and fixed with cold 80% ethanol for 1 hour on ice. Fixed cells were washed with staining buffer (0.2% Triton X-100 and 1 mmol/L EDTA, pH 8.0, in PBS) and resuspended in the staining buffer containing 50 ug/ml RNase A (Sigma-Aldrich, St. Louis, MO) and 50 ug/ml propidium iodide for 1 hour. Cell-cycle analysis was performed by FACS Caliber (BD Biosciences, Franklin Lakes, NJ, USA) using Cellquest analysis and specific S phase was analyzed using Modfit DNA Analysis (Verity Software House Inc, Topsham, ME, USA). For microarray analysis, RNA was extracted using RNeasy (Quiagen, Hilden, Germany) and analysed using Gene 1.0 ST Array (Affimetrix, Santa Clara, CA, USA). Results were examined using DAVID Bioinformatic Resources 6.7 (Frederick, MD, USA) and String protein association network software V9.0 (24).

Human tumor studies

Case selection, tissue microarray construction and image analyses—Following institutional ethics board approval, 153 cases of pheochromocytomas/paragangliomas were identified in our institutional files from 2001–2009. Of these, 132 tumors (82 paragangliomas, 43 pheochromocytomas and 7 metastases) from 115 patients provided enough tissue for tissue microarray construction. Triplicate or quadruplicate cores of tumor and normal adrenal medulla (when available) were included in the tissue microarray. Relevant clinical and histopathological data were recorded. tissue microarrays were stained with antibodies against FGFR1 (Abcam, Cambridge, MA, USA), FGFR2 (SC-122, Santa Cruz Biotechnology, Santa Cruz, CA, USA), FGFR3 (SC-123, Santa Cruz Biotechnology), FGFR4 (SC-124, Santa Cruz Biotechnology), c-KIT (A4502, Dako, Carpinteria, CA, USA), PDGFR α (Abcam, ab-61219), PDGFR β (sc-432, Santa Cruz Biotechnology), VEGFR1 (1301-1, Epitomics, Burlingame, CA, USA), VEGFR2 (2479, Cell Signaling, Beverly, MA, USA), SDHB (HPA002868; Sigma-Aldrich Corp), MIB1 (Novus Biologicals, Littleton, CO, USA, NB-110-90592), p16 (CINtect Histology Kit, Heidelberg, Germany), p21 (PharMingen, San Diego, CA, USA, 556431), p27 KIP1 (BD Transduction Laboratories, 610242), p53 (Novocastra, Newcastle, UK), Ki67 (Novus Biologicals), Cyclin D1 (Lab Vision, Fremont, CA, USA), Rb (PharMingen) and SDHB (Sigma-Aldrich Corp). Immunohistochemistry stained slides were scanned using ScanScope (Aperio, Vista, CA, USA) and analyzed using Spectrum Plus (Aperio) with algorithms to determine nuclear, membrane, cytoplasmic and overall immunostaining. Outputs generated included the percentage of positive nuclei and nuclear intensity score ranging from 0–3, according to the

average intensity of positive nuclei; the percentage of cells with positive membrane staining and a membrane final score ranging from 0–3 according to the percentages of strong, moderate and weak staining cells; and an overall staining score calculated by giving different weights to the percentage areas of weak, medium and strong immunostaining [$1*(\%Weak) + 2*(\%Medium) + 3*(\%Strong)$]. Unless otherwise specified, the use of the term “score” throughout the text refers to the overall staining score. All algorithms were optimized to ensure that the outputs generated corresponded to the pathologist interpretation of the immunostaining intensity and percentage.

Tumors with either completely negative staining or weak positivity for SDHB by immunohistochemistry were considered SDHB-deficient tumors. These are referred to as *SDH*-related, in accordance with the fact that they can be due to either mutations or epigenetic changes in *SDHA*, *SDHB*, *SDHC* or *SDHD*, or in genes involved in mitochondrial respiratory complex II assembly or regulation (22).

Immunohistochemistry Heat Maps and Hierarchical Clustering—The heat maps were generated using Multiple Experiment Viewer (MeV) software version 4.8.1 (25). The parameter settings for hierarchical clustering were based on the Pearson correlation distance metric, and the average linkage method. Rows represent the type of tumor and its genetic background. Columns represent the immunohistochemical stains. Green indicates the lowest expression, black indicates intermediate expression, and red indicates the highest expression of the overall immunohistochemistry score given for each tumor sample. The color scale bar is shown at the top of the heat maps.

FGFR4 genotyping—DNA was extracted using the phenol-chlorophorm method from paraffin cores collected at the time of tissue microarray construction. Whenever available, preference was given to normal tissue DNA (adjacent adrenal, lymph nodes or tissue available from other samples from the same patient). Exon 9 of *fgfr4* was PCR amplified and RFLP digested with *Bst*N1 to distinguish three *FGFR4* genotypes: wild type (Gly/Gly), heterozygous Gly³⁸⁸ (Gly/Arg) and homozygous Arg³⁸⁸ (Arg/Arg) as previously described (23).

Statistical Analyses

Continuous variables are expressed as mean plus minus standard deviation. Categorical variables are expressed as the absolute number and percentages. Comparisons between two continuous variables were performed using the Mann-Whitney test or the t-test. For comparisons between categorical variables the Chi-square test or the Fischer’s exact test were used, according to the distribution of the variable. Correlations between continuous variables were tested using the Pearson’s correlation coefficient. Univariate logistic regression analysis was used to determine if clinical characteristics, *FGFR4* genotypes and levels of expression of RTKs were predictors of the outcomes - death, metastasis or local recurrence. Odds ratios and 95% confidence intervals were estimated as measures of the magnitude of the associations. All analyses were carried out considering pheochromocytoma cases and paraganglioma cases separately. A p value < 0.05 was considered significant. Statistical analyses were performed using the SPSS 16.0 software (Chicago, IL, USA).

RESULTS

Cell line treatment analyses

Cell-cycle analysis showed that sunitinib decreases MPC 4/30 proliferation and increases apoptosis (Figure 1A). Gene expression profiling revealed that sunitinib strongly down-regulates cell cycle-associated genes. DAVID functional annotation tool analysis revealed that in tumor cells treated with sunitinib, approximately 37% of all genes (125/339) with >2-fold downregulation, are linked to the cell cycle (Supplemental table 1), of which more than 50% affect the M phase (summarized in Figure 1B as a gene interaction network). Of genes upregulated >2x by sunitinib, stress response proteins were some of the most prominently involved (12/63 proteins or 19%), (Supplemental table 2). A summary of the biological processes affected by sunitinib treatment *in vitro* is depicted in Figure 1C.

Clinical and histopathological data, outcomes and SDH status

Of 115 patients, 39 had pheochromocytomas and 76 had paragangliomas. According to the clinical notes, eight patients had MEN2, two patients had Neurofibromatosis type 1 and two patients had von Hippel-Lindau Syndrome; 46 cases showed SDHB loss by immunohistochemistry. Their main clinical and histopathological characteristics and *FGFR4* genotypes are summarized in Table 1. Additional tumor characteristics (location, size and weight,) are described in Supplemental table 3.

No association was found between age, gender or family history and the outcomes. Median follow-up was 23 months. Of the 9 malignant cases, 6 were SDHB-deficient. SDHB-intact and -deficient tumors differed significantly in several of the parameters analysed (Figure 2).

Sunitinib Targets Expression in Pheochromocytomas and Paragangliomas and Clinical Associations

Differential expression of the sunitinib targets VEGFR1 and 2, PDGFR α and β in pheochromocytomas, paragangliomas and normal medulla is depicted in Figures 3 and 4, and Supplemental Figures 1 to 3. Hierarchical clustering of tumors based on an immunohistochemistry heat map showed distinct segregation of pheochromocytomas from paragangliomas. *SDH*-related tumors tend to cluster together, as well as MEN2-associated tumors, which tended to have lower levels of VEGFRs.

C-KIT expression was low in both tumor types and did not differ significantly from normal medulla (Supplemental Figure 1).

VEGFR1 score was higher in paragangliomas, in males (128.3 vs. 111.1 \pm 42.8, $p=0.025$) and *SDH*-related tumors (Figures 2 and 4), but lower in pheochromocytomas (Figures 3 and 4). Overall staining and membrane scores were higher in tumors that metastasized (152.3 vs. 111, $p=0.01$ and 1.8 vs. 1.3 \pm , $p=0.022$, respectively) and were associated with increased risk of metastases (OR=1.05; 95% CI=1.01–1.10; $p=0.021$ for VEGFR1 score and OR=8.01; 95% CI=1.13–56.80; $p=0.037$ for VEGFR1 membrane score).

VEGFR2 was overexpressed in both tumor types (Figures 3 and 4), but tumors that metastasized had lower scores (67.4 vs. 90.0, $p=0.011$). It was associated with a decreased risk of metastasis (OR= 0.97, 95% CI=0.94–0.99, $p=0.017$).

PDGFR α score was higher in both tumor types (Figures 3 and 4) and in tumors that metastasized (73.5 vs. 53.2, $p=0.005$). PDGFR α membrane score was higher in tumors that metastasized (1.6 vs. 1.3, $p=0.008$), or died of the disease (2.0 vs. 1.2, $p=0.003$). It was associated with a significantly increased risk for metastasis (OR= 13.71, 95% CI=1.65–113.81, $p=0.015$).

PDGFR β score was higher in paragangliomas (Figures 3 and 4), *SDH*-related tumors (Figures 2 and 4) and tumors that metastasized (23.0 vs. 13.0, $p=0.032$). It was also higher in tumors from patients with a positive family history of pheochromocytoma/paraganglioma (22.5 vs. 12.9, $p=0.0031$), patients with *FGFR4* Gly/Gly genotype (17.2 vs. 11.7 in Gly/Arg patients, $p=0.045$) and was associated with an increased risk of metastasis (OR=1.04, 95% CI=1.01–1.09, $p=0.043$).

C-KIT levels were significantly lower in *SDH*-related tumors (Figure 2) and those that metastasized (13.7 vs. 24.1, $p=0.033$).

FGFR1, 2, 3 and 4 Expression in Pheochromocytomas and paragangliomas and Clinical Associations

FGFR1, 2 and 4 scores were higher in pheochromocytomas and paragangliomas compared to normal medulla (Figure 3). FGFR1, 2, and 4 expression was also higher in *SDH*-related tumors (Figure 2). In contrast, FGFR3 was overexpressed in pheochromocytomas but underexpressed in paragangliomas (Figures 3 and 4) and showed lower levels in *SDH*-related tumors (Figure 2). Additional data including membrane and nuclear differential expression of FGFRs in pheochromocytomas and paragangliomas can be found in Supplemental Figure 4.

FGFR1 score was higher in tumors that metastasized (117.5 vs. 94; $p=0.01$) and was associated with increased risk for metastases (OR=1.03; 95% CI=1.01–1.05; $p=0.027$). FGFR2 nuclear score was higher in tumors that metastasized (1.7 vs. 1.3; $p=0.002$) and was associated with increased risk of metastasis (OR=7.61; 95% CI=1.70–34.17; $p=0.008$). Conversely, FGFR3 score was significantly lower in tumors that metastasized (31.3 vs. 49.0; $p=0.006$). In paragangliomas, an inverse correlation was found between the tumor size and the percentage and intensity of FGFR3 membrane staining ($r=-0.364$, $p=0.001$ and $r=-0.277$, $p=0.022$). FGFR4 score was higher in tumors from patients with a positive family history of pheochromocytoma/paraganglioma (24.6 vs. 13.7; $p=0.002$). A positive correlation between tumor size and FGFR4 percentage and intensity of membrane staining was present in paragangliomas ($r=0.240$, $p=0.38$ and $r=0.260$, $p=0.024$ respectively), while a positive correlation between the FGFR4 overall staining score and MIB1 percent positive nuclei was observed in pheochromocytomas ($r=0.359$, $p=0.025$).

FGFR4 genotyping of Pheochromocytomas and Paragangliomas and Clinical Associations

From 115 patients, DNA was extracted from either normal (N=107) or tumor (N=8) tissue. In 9 cases, genotyping could not be performed. There was no significant difference in the distribution of these alleles between pheochromocytomas and paragangliomas (Table 1). No association was found between *FGFR4* genotype and FGFR4 levels of expression, nor with age, gender, bilateral/multiple tumors, family history, any individual outcomes or the combined outcome.

A comparison between the distribution of *FGFR4* alleles in our cases and those of normal populations previously reported in the literature is depicted in Table 2.

Cell Cycle Markers in Pheochromocytomas and Paragangliomas and Clinical Associations

The differential expression of cell cycle markers in pheochromocytomas, paragangliomas and normal medulla is depicted in Figure 5, with selected markers also shown in Figure 4 and additional outputs analysed in Supplemental Figure 5. Aurora B expression was negligible (not shown). Cell cycle marker expression according to the SDHB immunohistochemistry status of tumors is illustrated in Figure 2.

Tumors that metastasized had a higher percentage of cytoplasmic p27 staining (53.5% vs. 39.1%, $p=0.045$) and MIB1 percent positive nuclei (5.8% vs 2.5%, $p=0.002$). MIB1 labelling index (LI) was associated with increased risk of metastasis (OR=1.26, 95%CI=1.06–1.49, $p=0.008$).

Tumors from patients with a family history of pheochromocytoma/paraganglioma had a higher p16 score (50.75 vs. 28.1, $p=0.033$) and a higher percentage of p16 cytoplasmic staining (30.7% vs. 11.5%, $p=0.002$). Bilateral or multiple tumors had a higher percentage of Rb positive nuclei (95.6% vs. 91.2%; $p=0.033$).

Tumors from patients carrying an *FGFR4*-R388 allele had a higher percentage of nuclei positive for p53 (2.1% vs. 1%, $p=0.014$) and a lower percentage for Cyclin D1 (60.9% vs. 70.6%, $p=0.002$).

DISCUSSION

Sunitinib potential targets in Pheochromocytomas and Paragangliomas

We have demonstrated that sunitinib treatment decreases cell proliferation in mouse pheochromocytoma cells *in vitro* mainly by affecting cell cycle, DNA metabolism, and cell organization genes. It also increases apoptosis, which is in keeping with similar observations of sunitinib treatment of a rat pheochromocytoma cell line (19).

Among sunitinib potential targets, VEGFR2 and PDGFR α were overexpressed in pheochromocytomas and paragangliomas, while PDGFR β was overexpressed in paragangliomas only and VEGFR1 was overexpressed in paragangliomas but underexpressed in pheochromocytomas. Membranous PDGFR α and VEGFR1 were associated with an increased risk of metastatic disease. Our finding of high VEGFR levels in these tumors is consistent with previous observations (12–14). In addition, VEGF (13, 14)

and VEGFR1 (14) overexpression might be predictors of malignant behavior. Given that VEGF/VEGFR expression are regulated by HIF1 α and HIF2 α , it is not surprising that we found higher levels of VEGFR1 in SDHB deficient tumors, which is also in keeping with previous studies showing a high expression of angiogenic markers in *SDH*- and *VHL*-related tumors (14). VEGFR1 expression has also been associated with poor prognostic features in thyroid (26) and hepatocellular carcinoma (27).

The role of PDGFRs and their ligands in human malignancies is well documented (28). In papillary thyroid cancer, PDGFR α overexpression was associated with lymph node metastasis (29), and in prostate adenocarcinomas, PDGFR α expression was associated with bone metastasis (30). PDGF receptors, particularly PDGFR α , have been implicated in neural crest cell (NCC) migration and NCC-derived tissue development (31). PDGFs expression in cultured cells is responsive to a variety of stimuli, including hypoxia (28). Since at least a subset of pheochromocytomas (*SDH*-related and *VHL*-associated tumors) exhibits a hypoxic gene signature, it is possible that an autocrine-paracrine PDGF-PDGFR loop might be in place in these tumors, as is the case with other human malignancies (28). That would be in keeping with our observation of higher PDGFR β overall staining score in *SDH*-related tumors. Moreover, bFGF stimulates PDGFR α expression in smooth muscle cells *in vitro* (32). Overexpression of bFGF in paragangliomas (3, 15) could potentially contribute to PDGFR α overexpression and explain the positive correlation observed between expression of PDGFR α and the bFGF receptor FGFR1. Both are involved in the proliferation of oligodendrocyte progenitors in response to demyelination (33).

Low expression of C-KIT is consistent with previous reports of lack of response of pheochromocytomas to C-KIT inhibitor therapy (34).

FGFRs in Pheochromocytomas and Paragangliomas

FGFR1, -2 and -4 are overexpressed in pheochromocytomas and paragangliomas; FGFR1 score and FGFR2 nuclear score were associated with an increased risk of metastasis. Even though there was no significant association between FGFR4 levels and outcomes, there was a positive correlation between FGFR4 levels and MIB1 LI in pheochromocytomas and with tumor size and weight in paragangliomas.

These findings suggest that FGFRs 1, 2 and 4 may be involved in pheochromocytoma/paraganglioma progression; this is supported by the observation that bFGF can act as a mitogen for rat chromaffin cells, especially in low oxygen concentrations or when associated with insulin-like growth factors (35, 36), and can promote survival in rat pheochromocytoma PC12 cells (15). Additionally, bFGF levels are higher in pheochromocytomas and paragangliomas than in normal adrenal medulla (3, 15); both bFGF and FGFR1 are expressed in pheochromocytomas and at higher levels than in normal carotid body, pointing to a possible autocrine or paracrine mechanism for tumor development (16). We identified a higher FGFR1 score in *SDH*-related tumors; Dekker et al also showed higher staining intensity of FGFR1 and higher bFGF RNA levels in *SDHD* mutated *versus* sporadic tumors (16).

A role for FGFRs in carcinogenesis and tumor progression has been well documented in various human malignancies, including prostate, colon, lung, breast and bladder cancer; multiple myeloma and sarcomas (37). FGFR1 overexpression has been associated with liver metastasis in colorectal carcinoma (38).

FGFR2 is more controversial as an oncogene (37), since in some models, such as pituitary (10) and thyroid (8), it may act as a tumor suppressor. This might in part be due to alternative gene splicing that generates two common FGFR2 isoforms which have different binding affinities to FGFs and are differentially expressed in normal tissues and tumors. Many tumors have shown a switch from the FGFR2 isoform expressed in their normal tissue of origin (37). Moreover, the same FGFR2 isoform may have different properties that vary with the cell in which it is expressed (tumor epithelial *versus* stromal cells), and the interaction between these is what will determine net effect of FGFR2 isoforms on a specific tumor growth and progression (8).

Our finding that nuclear FGFR2 was associated with increased risk of metastasis and recurrence is not unprecedented. FGFRs can localize to the nucleus in normal and neoplastic cells (39), including those of the adrenal medulla (40, 41). Nuclear FGFRs may be crucial in malignant transformation, as exemplified in a breast cancer model where FGFR1 activates genes involved in cell migration (39). Thus, both the isoform(s) expressed and the intracellular location of FGFRs seems to be important. However further investigation is required to determine the FGFR2 isoforms expressed in pheochromocytomas and paragangliomas.

Approximately 60% of patients in our series harbored the *FGFR4*-R388 SNP allele. Compared to normal population distributions (Table 2), there is a clear over-representation of this genotype in our patient population. Nevertheless, in contrast with other malignancies (17), there was no significant association between genotype and clinical characteristics or outcomes. This may be due to the relatively small sample size, and to the low frequency of negative outcomes in our series. A higher FGFR4 score was found in familial and *SDH*-related tumors.

In contrast to FGFRs 1, 2 and 4, FGFR3 was underexpressed in paragangliomas, while overexpressed in pheochromocytomas. FGFR3 expression was significantly lower in tumors that metastasized, with high levels of FGFR3 being associated with a decreased risk of aggressive behavior. Membranous FGFR3 expression was inversely correlated with tumor size in paragangliomas. All these point to a tumor suppressive role for FGFR3 in pheochromocytomas and paragangliomas, which is supported by the association of FGFR3 overexpression/mutation with better prognosis in bladder (42), and prostate carcinomas (43).

Cell Cycle Markers in Pheochromocytomas and Paragangliomas

Given the well known indolent growth of both pheochromocytomas and paragangliomas, overexpression of cell cycle inhibitors is not unexpected. Malignant tumors showed a higher MIB1 LI consistent with previous studies (3, 4), and also a higher percentage of p27 cytoplasmic staining, which has not been previously reported in pheochromocytomas and paragangliomas.

While p27 has been traditionally viewed as a tumor suppressor gene due to its ability to block cell cycle progression, there is increasing evidence that its role in tumorigenesis may go beyond cell cycle regulation. Cytoplasmic relocalization has been shown to be one of the mechanisms tumor cells develop to inactivate p27. In the cytoplasm, p27 not only cannot exert its inhibitory actions over cyclin-CDKs, but may also actively participate in the process of malignant transformation (44). In keeping with that, cytoplasmic p27 has been associated with poor prognosis in carcinomas of the breast, cervix, esophagus, ovary, uterus, some leukemias and lymphomas, and in melanomas (44).

The low percentage of p53 staining is in accordance with previous studies showing a very low frequency of p53 mutations in these tumors (45).

Interestingly, while p21, p27, Cyclin D1 and Rb levels were higher in *SDH*-related tumors, p16 showed the reverse pattern. These findings are consistent with a previous report of p16^{INK4a} promoter hypermethylation in *SDHB* mutated and malignant tumors (46) and with the observation that pheochromocytoma-prone mice with homozygous *Ink4a/Arf* inactivation often develop malignant tumors (46).

Aurora kinases are serine/threonine kinases that, together with cyclin-dependent kinases and Polo-like kinases, are essential for proper progression of cell division through mitoses (47). Aurora A overexpression may contribute to genetic instability by disrupting the proper assembly of the mitotic checkpoint complex and has been detected in breast, colorectal, bladder, pancreatic, gastric, ovarian and esophageal cancers (47). No studies have thus far described the expression of Aurora kinases in pheochromocytomas and paragangliomas. We show that Aurora A is underexpressed in paragangliomas when compared to normal medulla and that Aurora B expression is negligible in both tumors. This is consistent with the fact that most pheochromocytomas and paragangliomas have overall low levels of genetic instability (48) and suggests that these tumors are not a suitable target for specific Aurora Kinase inhibitor therapy.

Our findings provide novel insights into mechanistic actions of Sunitinib in pheochromocytomas and paragangliomas and give support to current evidence that multitargeted TKIs might be a suitable treatment alternative for pheochromocytomas and paragangliomas.

Immunohistochemical Heat Maps and Hierarchical Clustering

Hierarchical clustering based on the immunohistochemistry heat maps generated from our samples was consistent with previous observations that pheochromocytomas and paragangliomas, although sharing the same embryological origin, are a heterogeneous group of tumors that are better subclassified by their gene expression profiling (14, 49). These studies have shown that pheochromocytomas and paragangliomas consistently segregate into two clusters, one characterized by a pseudo-hypoxic gene signature and comprising *VHL* and *SDH*-related tumors; and the other including MEN and NF1 associated tumors, as well as most sporadic samples (14). In accordance with those previous studies, we have observed that *SDH*-related tumors show higher VEGFR1 and 2 levels when compared to MEN2 tumors, consistent with a so-called “pseudo-hypoxic” gene signature in that cluster.

The consistency of our findings with those previously reported in the literature not only helps to validate the use of automated immunohistochemistry analyses in our study but also the use of SDHB immunohistochemistry as an initial screening tool for identifying *SDH*-related tumors.

Supplementary Material

Refer to Web version on PubMed Central for supplementary material.

Acknowledgments

We kindly thank Dr A. Tischler for providing the MPC 4/30 cell line and Dr J. Powers for his support and assistance in growing MPC cells.

Clarissa Araujo Cassol was a recipient of the grant “Strategic Training in Health Research (STIHR), STP-53912” at the time this research was conducted.

References

1. Lloyd, RV., Tischler, AS., Kimura, N., McNicol, AM., Young, WF, Jr. Adrenal tumors: introduction. In: DeLellis, RA.Lloyd, RV.Heitz, PU., Eng, C., editors. Pathology and genetics of tumours of endocrine organs. World Health Organization classification of tumours. IARC Press; Lyon, France: 2004. p. 137-138.
2. Gimenez-Roqueplo AP, Tischler AS. Pheochromocytoma and Paraganglioma: Progress on all fronts. *Endocr Pathol.* 2012; 23:1–3. [PubMed: 22246920]
3. Clarke MR, Weyant RJ, Watson CG, Carty SE. Prognostic markers in pheochromocytoma. *Hum Pathol.* 1998; 29:522–6. [PubMed: 9596278]
4. August C, August K, Schroeder S, et al. CGH and CD 44/MIB-1 immunohistochemistry are helpful to distinguish metastasized from nonmetastasized sporadic pheochromocytomas. *Mod Pathol.* 2004; 17:1119–28. [PubMed: 15167935]
5. Ayala-Ramirez M, Feng L, Johnson MM, et al. Clinical risk factors for malignancy and overall survival in patients with pheochromocytomas and sympathetic paragangliomas: Primary tumor size and primary tumor location as prognostic indicators. *J Clin Endocrinol Metab.* 2011; 96:717–25. [PubMed: 21190975]
6. Joshua AM, Ezzat S, Asa SL, et al. Rationale and Evidence for Sunitinib in the Treatment of Malignant Paraganglioma/Pheochromocytoma. *J Clin Endocrinol Metab.* 2009; 94:5–9. [PubMed: 19001511]
7. Ayala-Ramirez M, Chougnet CN, Habra MA, et al. Treatment with sunitinib for patients with progressive metastatic pheochromocytomas and sympathetic paragangliomas. *J Clin Endocrinol Metab.* 2012; 97:4040–50. [PubMed: 22965939]
8. Guo M, Liu W, Serra S, Asa SL, Ezzat S. FGFR2 isoforms support epithelial-stromal interactions in thyroid cancer progression. *Cancer Res.* 2012; 72:2017–27. [PubMed: 22345151]
9. Kondo T, Zheng L, Liu W, Kurebayashi J, Asa SL, Ezzat S. Epigenetically controlled fibroblast growth factor receptor 2 signalling imposes on the RAS/BRAF/mitogen-activated protein kinase pathway to modulate thyroid cancer progression. *Cancer Res.* 2007; 67:5461–70. [PubMed: 17545628]
10. Zhu X, Asa SL, Ezzat S. Fibroblast growth factor 2 and estrogen control the balance of histone 3 modifications targeting MAGE-A3 in pituitary neoplasia. *Clin Cancer Res.* 2008; 14:1984–96. [PubMed: 18381936]
11. Serra S, Zheng L, Hassan M, et al. The *FGFR4*-G388R single-nucleotide polymorphism alters pancreatic neuroendocrine tumor progression and response to mTOR inhibition therapy. *Cancer Res.* 2012; 72:5683–91. [PubMed: 22986737]

12. Takekoshi K, Isobe K, Yashiro T, et al. Expression of vascular endothelial growth factor (VEGF) and its cognate receptors in human pheochromocytomas. *Life Sciences*. 2004; 74:863–71. [PubMed: 14659975]
13. Salmenkivi K, Heikkilä P, Liu J, Haglund C, Arola J. VEGF in 105 pheochromocytomas: enhanced expression correlates with malignant outcome. *APMIS*. 2003; 111:458–64. [PubMed: 12780519]
14. Favier J, Igaz P, Burnichon N, et al. Rationale for anti-angiogenic therapy in pheochromocytoma and paraganglioma. *Endocr Pathol*. 2012; 23:34–42. [PubMed: 22183643]
15. Statuto M, Ennas MG, Zamboni G, et al. Basic fibroblast growth factor in human pheochromocytoma: a biochemical and immunohistochemical study. *Int J Cancer*. 1993; 53:5–10. [PubMed: 8380057]
16. Dekker PBD, Kuipers-Dijkshoorn NJ, Baelde HJ, van der Mey AGL, Hogendoorn PCW, Cornelisse CJ. Basic fibroblast growth factor and fibroblastic growth factor receptor-1 may contribute to head and neck paraganglioma development by an autocrine or paracrine mechanism. *Human Pathology*. 2007; 38:79–85. [PubMed: 16949906]
17. Xu W, Li Y, Wang X, et al. *FGFR4* transmembrane domain polymorphism and cancer risk: a meta-analysis including 8555 subjects. *Eur J Cancer*. 2010; 46:3332–8. [PubMed: 20638838]
18. Ellis LM, Hicklin DJ. VEGF-targeted therapy: mechanisms of anti-tumour activity. *Nat Rev Cancer*. 2008; 8:579–91. [PubMed: 18596824]
19. Saito Y, Tanaka Y, Aita Y, et al. Sunitinib induces apoptosis in pheochromocytoma tumor cells by inhibiting VEGFR2/Akt/mTOR/S6K1 pathways through modulation of Bcl-2 and BAD. *Am J Physiol Endocrinol Metab*. 2012; 302:E615–25. [PubMed: 21878661]
20. Powers JF, Evinger MJ, Tsokas P, et al. Pheochromocytoma cell lines from heterozygous neurofibromatosis knockout mice. *Cell Tissue Res*. 2000; 302:309–20. [PubMed: 11151443]
21. Kono SA, Marshall ME, Ware KE, Heasley LE. The fibroblast growth factor receptor signaling pathway as a mediator of intrinsic resistance to EGFR-specific tyrosine kinase inhibitors in non-small cell lung cancer. *Drug Resist Updat*. 2009; 12:95–102. [PubMed: 19501013]
22. van Nederveen FH, Gaal J, et al. An immunohistochemical procedure to detect patients with paraganglioma and pheochromocytoma with germline *SDHB*, *SDHC*, or *SDHD* gene mutations: a retrospective and prospective analysis. *Lancet Oncol*. 2009; 10:764–71. [PubMed: 19576851]
23. Bange J, Prechtel D, Cheburkin Y, et al. Cancer progression and tumor cell motility are associated with the *FGFR4* Arg(388) allele. *Cancer Res*. 2002; 62:840–7. [PubMed: 11830541]
24. Jensen LJ, Kuhn M, Stark M, et al. STRING 8 - a global view on proteins and their functional interactions in 630 organisms. *Nucleic Acids Res*. 2009; 37:D412–6. [PubMed: 18940858]
25. Saeed AI, Sharov V, White J, et al. TM4: a free, open-source system for microarray data management and analysis. *Biotechniques*. 2003; 34:374–8. [PubMed: 12613259]
26. Karaca Z, Tanriverdi F, Unluhizarci K, et al. VEGFR1 expression is related to lymph node metastasis and serum VEGF may be a marker of progression in the follow-up of patients with differentiated thyroid carcinoma. *Eur J Endocrinol*. 2011; 164:277–84. [PubMed: 21097568]
27. Li T, Zhu Y, Qin CY, et al. Expression and prognostic significance of vascular endothelial growth factor receptor 1 in hepatocellular carcinoma. *J Clin Pathol*. 2012; 65:808–14. [PubMed: 22734007]
28. Heldin CH. Autocrine PDGF stimulation in malignancies. *Ups J Med Sci*. 2012; 117:83–91. [PubMed: 22512244]
29. Zhang J, Wang P, Dykstra M, et al. Platelet-derived growth factor receptor- α promotes lymphatic metastases in papillary thyroid cancer. *J Pathol*. 2012; 228:241–50. [PubMed: 22744707]
30. Russell MR, Liu Q, Fatatis A. Targeting the alpha receptor for platelet-derived growth factor as a primary or combination therapy in a preclinical model of prostate cancer skeletal metastasis. *Clin Cancer Res*. 2010; 16:5002–10. [PubMed: 20813817]
31. Smith CL, Tallquist MD. PDGF function in diverse neural crest cell populations. *Cell Adh Migr*. 2010; 4:561–6. [PubMed: 20657170]
32. Schöllmann C, Grugel R, Tatje D, et al. Basic fibroblast growth factor modulates the mitogenic potency of the platelet-derived growth factor (PDGF) isoforms by specific upregulation of the PDGF alpha receptor in vascular smooth muscle cells. *J Biol Chem*. 1992; 267:18032–9. [PubMed: 1325456]

33. Frost EE, Nielsen JA, Le TQ, Armstrong RC. PDGF and FGF2 regulate oligodendrocyte progenitor responses to demyelination. *J Neurobiol.* 2003; 54:457–72. [PubMed: 12532397]
34. Koch CA, Gimm O, Vortmeyer AO, et al. Does the expression of c-kit (CD117) in neuroendocrine tumors represent a target for therapy? *Ann N Y Acad Sci.* 2006; 1073:517–26. [PubMed: 17102120]
35. Nurse CA, Vollmer C. Role of basic FGF and oxygen in control of proliferation, survival, and neuronal differentiation in carotid body chromaffin cells. *Dev Biol.* 1997; 184:197–206. [PubMed: 9133430]
36. Frödin M, Gammeltoft S. Insulin-like growth factors act synergistically with basic fibroblast growth factor and nerve growth factor to promote chromaffin cell proliferation. *Proc Natl Acad Sci USA.* 1994; 91:1771–5. [PubMed: 8127879]
37. Brooks AN, Kilgour E, Smith PD. Molecular pathways: fibroblast growth factor signaling: a new therapeutic opportunity in cancer. *Clin Cancer Res.* 2012; 18:1855–62. [PubMed: 22388515]
38. Sato T, Oshima T, Yoshihara K, et al. Overexpression of the fibroblast growth factor receptor-1 gene correlates with liver metastasis in colorectal cancer. *Oncol Rep.* 2009; 21:211–6. [PubMed: 19082464]
39. Chioni AM, Grose R. FGFR1 cleavage and nuclear translocation regulates breast cancer cell behavior. *J Cell Biol.* 2012; 197:801–17. [PubMed: 22665522]
40. Stachowiak MK, Maher PA, Joy A, Mordechai E, Stachowiak EK. Nuclear accumulation of fibroblast growth factor receptors is regulated by multiple signals in adrenal medullary cells. *Mol Biol Cell.* 1996; 7:1299–317. [PubMed: 8856671]
41. Peng H, Moffett J, Myers J, et al. Novel nuclear signalling pathway mediates activation of fibroblast growth factor-2 gene by type 1 and type 2 angiotensin II receptors. *Mol Biol Cell.* 2001; 12:449–62. [PubMed: 11179427]
42. van Rhijn BW, van der Kwast TH, Liu L, et al. The *FGFR3* mutation is related to favorable pT1 bladder cancer. *J Urol.* 2012; 187:310–4. [PubMed: 22099989]
43. Hernandez S, de MS, Agell L, et al. *FGFR3* mutations in prostate cancer: association with low-grade tumors. *Mod Pathol.* 2009; 22:848–56. [PubMed: 19377444]
44. Serres MP, Zlotek-Zlotkiewicz E, Concha C, et al. Cytoplasmic p27 is oncogenic and cooperates with Ras both in vivo and in vitro. *Oncogene.* 2011; 30:2846–58. [PubMed: 21317921]
45. Petri BJ, Speel EJ, Korpershoek E, et al. Frequent loss of 17p, but no *p53* mutations or protein overexpression in benign and malignant pheochromocytomas. *Mod Pathol.* 2008; 21:407–13. [PubMed: 18223555]
46. Kiss NB, Geli J, Lundberg F, et al. Methylation of the *p16INK4A* promoter is associated with malignant behavior in abdominal extra-adrenal paragangliomas but not pheochromocytomas. *Endocr Relat Cancer.* 2008; 15:609–21. [PubMed: 18509008]
47. Saeki T, Ouchi M, Ouchi T. Physiological and oncogenic Aurora-A pathway. *Int J Biol Sci.* 2009; 5:758–62. [PubMed: 20011137]
48. Sandgren J, Diaz de Ståhl T, Andersson R, et al. Recurrent genomic alterations in benign and malignant pheochromocytomas and paragangliomas revealed by whole-genome array comparative genomic hybridization analysis. *Endocr Relat Cancer.* 2010; 17:561–79. [PubMed: 20410162]
49. Dahia PL, Ross KN, Wright M, et al. A HIF1 alpha regulatory loop links hypoxia and mitochondrial signals in pheochromocytomas. *PLoS Genet.* 2005; 1:72–80. [PubMed: 16103922]

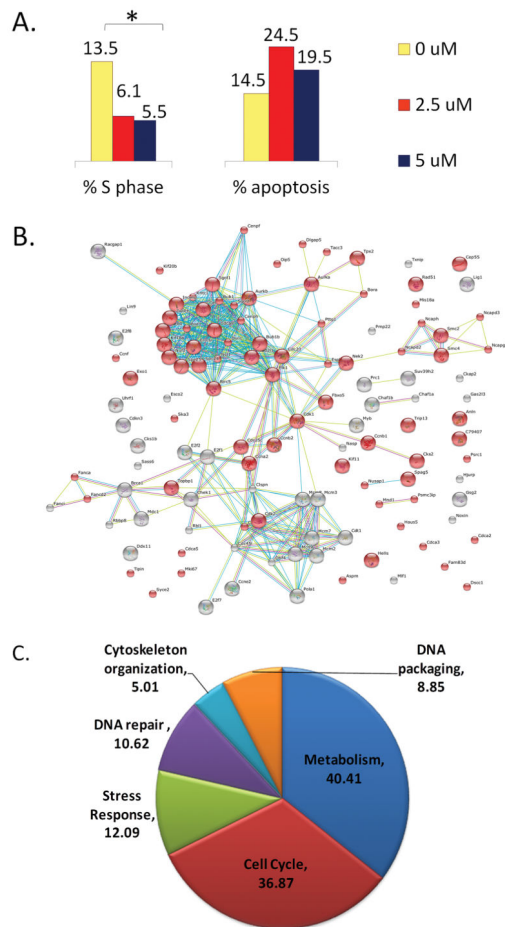


Figure 1. Sunitinib treatment of the mouse pheochromocytoma MPC 4/30 cell line in vitro
 A. Cell cycle analyses of MPC 4/30 cells treated with 2.5 and 5 μ M of sunitinib show a significant inhibition of replication compared with controls receiving 0 μ M (* $p < 0.05$). Values shown represent means derived from 3 different experiments. B. More than 50% of cell cycle proteins $>2X$ down regulated by sunitinib affect the M phase of mitosis. C. The major biological processes affected by sunitinib in MPC 4.30 cells are demonstrated.

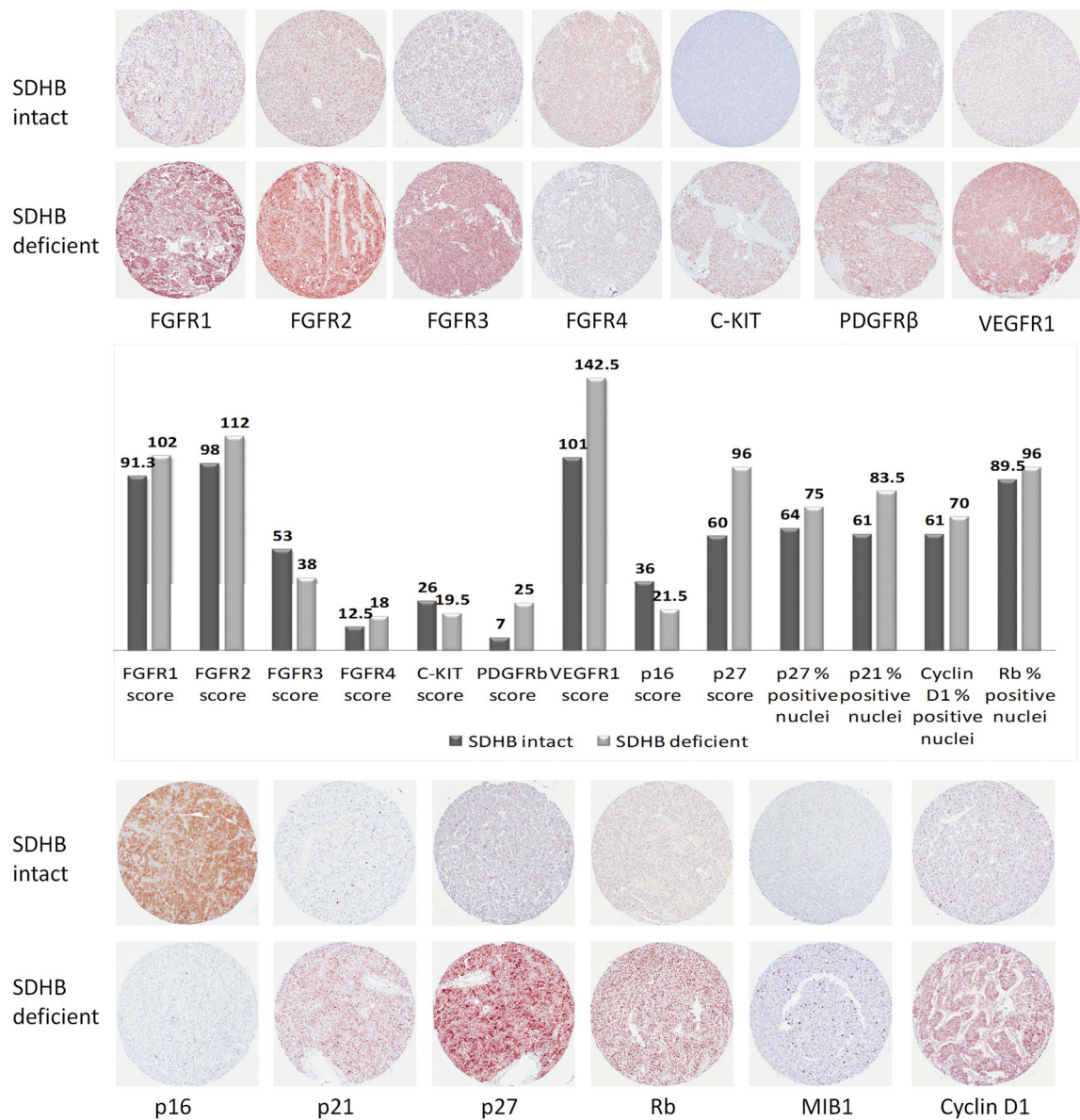


Figure 2. Differential expression of RTKs and cell cycle markers between SDHB-intact and SDHB-deficient tumors
 SDHB-deficient tumors (n=46) are considered to be *SDH*-related. Only significant results ($p < 0.05$) are shown, along with representative tissue microarray spots. Score refers to the overall staining score (values range: 0–300).

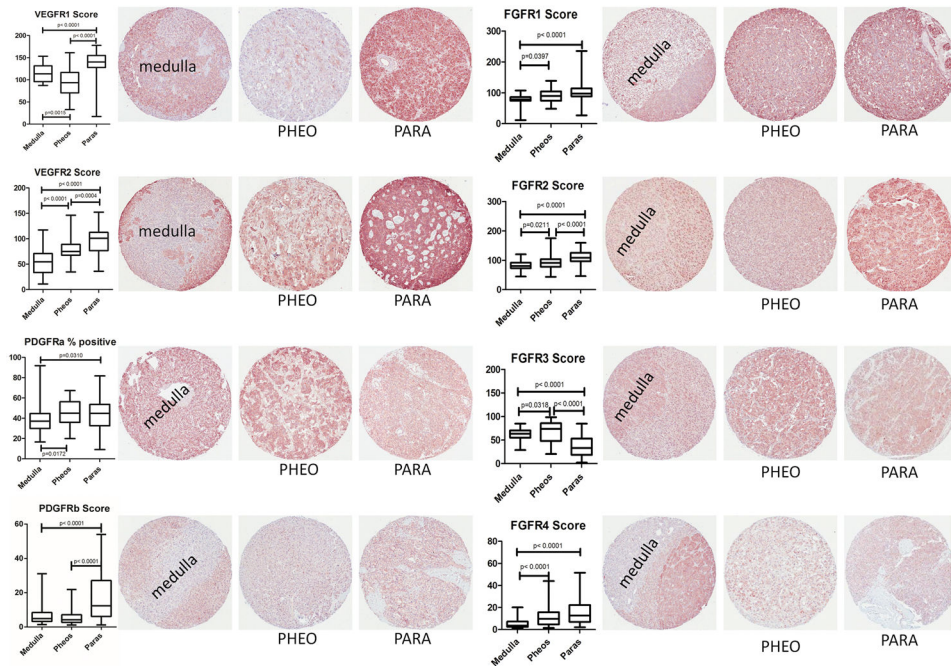


Figure 3. Expression of VEGFRs PDGFRs and FGFRs in pheochromocytomas, paragangliomas and normal adrenal medulla

Representative tissue microarray spots are shown and staining score values ranging from 0–300 are graphed. Pheos – pheochromocytomas; paras – paragangliomas.

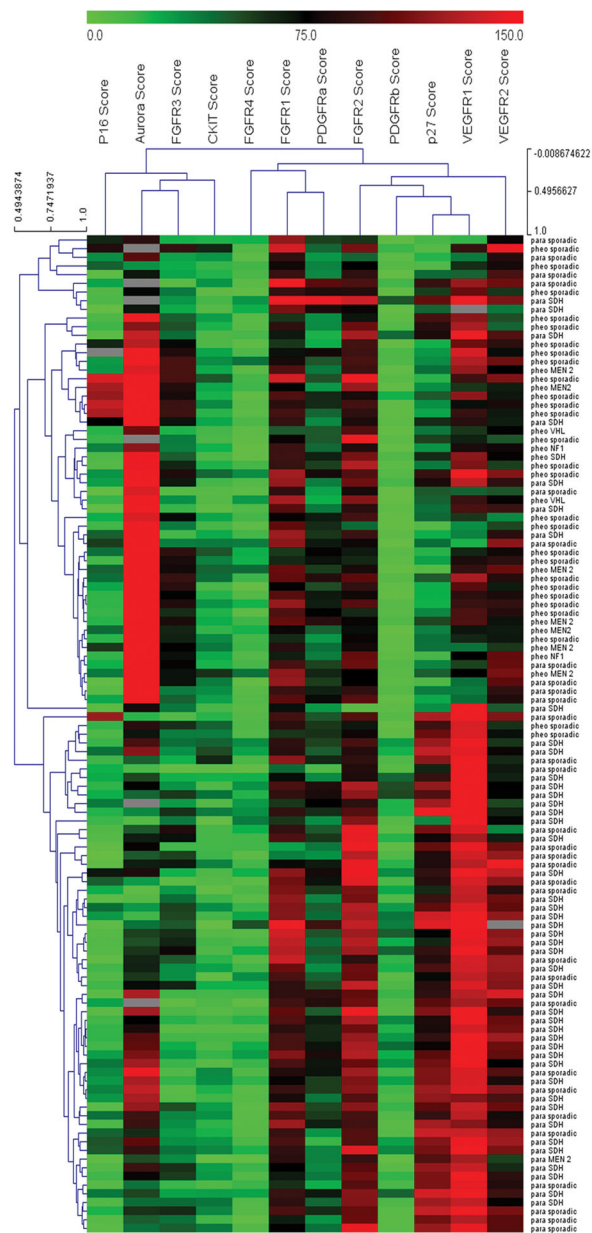


Figure 4. Heat Map Summary of Immunohistochemical expression of selected markers in Paragangliomas and Pheochromocytomas

Rows represent the type of tumor and its genetic background. Columns represent the immunohistochemical stains. Green indicates the lowest expression, black indicates intermediate expression, and red indicates the highest expression of the overall immunohistochemistry score given for each tumor sample. Pheo –pheochromocytoma; para – paraganglioma.

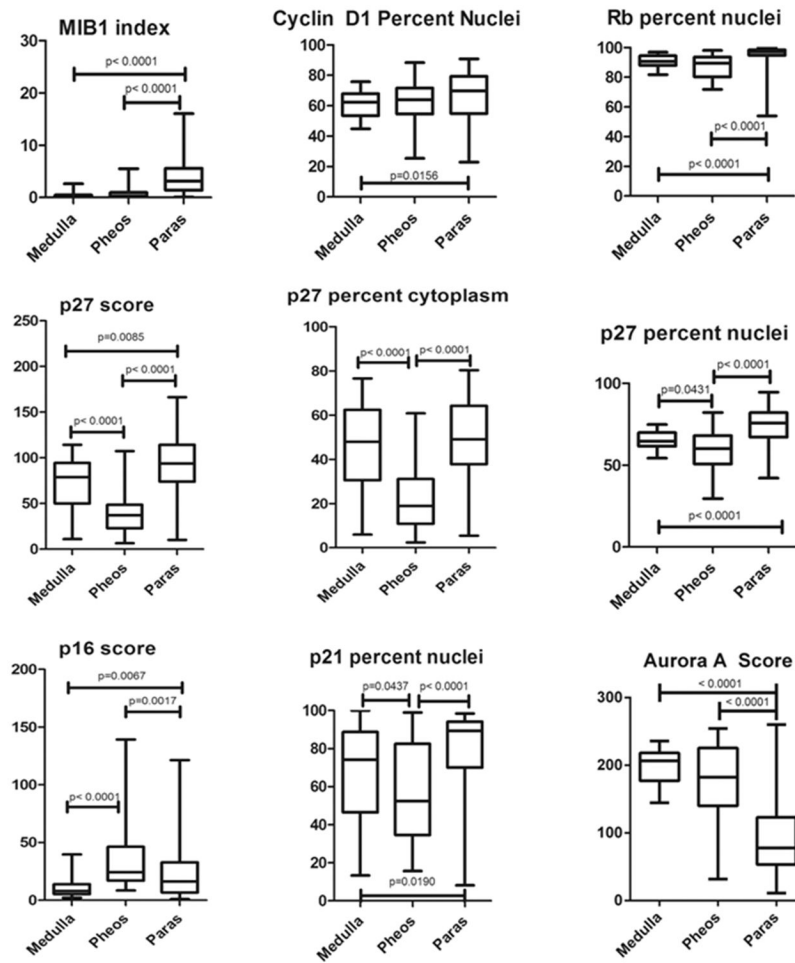


Figure 5. Differential expression of cell cycle markers in pheochromocytomas, paragangliomas and normal adrenal medulla

39 pheochromocytomas, 76 paragangliomas, and 35 normal human adult adrenomedullary tissue samples were compared. Unless otherwise specified, the heading “score” refers to the overall staining score (values range 0–300). MIB1 index refers to the percentage of nuclei staining for MIB1. Pheos – pheochromocytomas; paras – paragangliomas.

Table 1

Clinical Characteristics of Patients

| Variable | All patients (n=115) | Pheo (n=39) | Para (n=76) | p-value |
|--------------------------------|----------------------|-------------|-------------|---------|
| Age at diagnosis | 46.8± 12.3 | 45.9 ± 13.0 | 47.3 ± 12.0 | .571 |
| Female gender | 71 (61.7) | 22 (56.4) | 49 (64.5) | .424 |
| FGFR4 genotype (n=105) | | | | |
| G388-G388 (Gly/Gly) | 38 (33) | 9 (23.1) | 29 (38.2) | 0.64 |
| G388-R388 (Gly/Arg) | 68 (59) | 30 (76.9) | 38 (50) | |
| Unknown | 9 (7.8) | 0 (-) | 9 (11.8) | |
| SDHB loss by IHC | 46 (40) | 1 (2.6) | 45 (59) | <0.001 |
| Bilateral/multiple | 20 (17.4) | 4 (10.3) | 17 (22.4) | .132 |
| Family history | 10 (8.6) | 4 (10.3) | 5 (6.6) | .486 |
| Metastatic disease | 9 (7.8) | 0 (-) | 9 (11.8) | .093 |
| Local recurrence | 4 (3.5) | 0 (-) | 4 (5.3) | .298 |
| Death related to tumour | 2 (1.7) | 0 (-) | 2 (2.6) | .548 |

Values are means ± standard deviations. Numbers in brackets are percentage of an absolute number. N = number.

Table 2

Distribution of FGFR4 codon 388 SNP alleles in normal populations (18) and in patients with pheochromocytomas and paragangliomas from our series

| | Gly/Gly (%) | p-value | Gly/Arg (%) | p-value | Arg:Arg (%) | p-value |
|---------------------------|-------------|---------------|-------------|-----------------|-------------|-----------------|
| Present Study | 33 | | 59 | | 0 | |
| Bange 2002 | 45 | 0.0460 | 49 | 0.0015 | 6 | 0.002 |
| Morimoto 2003 | 38.2 | 0.8900 | 49 | 0.0432 | 12.7 | < 0.0001 |
| Wang 2004 | 54.6 | 0.0100 | 41.2 | 0.0017 | 4.1 | 0.03 |
| Spinola 2005 ¹ | 50.9 | 0.0170 | 37.3 | < 0.0001 | 11.4 | < 0.0001 |
| Spinola 2005 ² | 48.1 | 0.0400 | 41.9 | < 0.0001 | 10 | < 0.0001 |
| Yang 2008 | 32 | 0.3200 | 50.6 | 0.0176 | 17.4 | < 0.0001 |
| Ma 2008 | 37.4 | 1.0000 | 48.6 | 0.0188 | 14 | < 0.0001 |
| Han 2009 | 34.1 | 0.6000 | 43.2 | 0.0052 | 22.7 | < 0.0001 |
| FitzGerald 2009 | 50.4 | 0.0050 | 39.6 | < 0.0001 | 9.9 | < 0.0001 |
| Naidu 2009 | 52.4 | 0.0060 | 41.6 | < 0.0001 | 6 | 0.0002 |
| Tanuma 2010 | 42 | 0.0420 | 48 | 0.03 | 10 | < 0.0001 |
| Ho 2010 | 51.5 | 0.0070 | 40.2 | < 0.0001 | 8.2 | 0.003 |

Bold highlights significant values (p<0.05).